Icarus 211 (2011) 699–706

Contents lists available at ScienceDirect

Icarus

journal homepage: www.elsevier.com/locate/icarus

Hypsometry of Titan

Ralph D. Lorenz [a,*], Elizabeth P. Turtle [a], Bryan Stiles [b], Alice Le Gall [b], Alexander Hayes [c], Oded Aharonson [c], Charles A. Wood [d], Ellen Stofan [e], Randy Kirk [f]

[a] Space Department, Johns Hopkins University Applied Physics Laboratory, 11100 Johns Hopkins Road, Laurel, MD 20723, USA
[b] Jet Propulsion Laboratory, 4800 Oak Grove Drive, Pasadena, CA 91109, USA
[c] California Institute of Technology, 1200 East California Boulevard, Pasadena, CA 91125, USA
[d] Wheeling Jesuit University, Wheeling, VA 26003, USA
[e] USA Proxemy Research, Bowie, MD 20715, USA
[f] US Geological Survey, 2255 N. Gemini Dr., Flagstaff, AZ 86001, USA

ARTICLE INFO

Article history:
Received 30 March 2010
Revised 1 October 2010
Accepted 2 October 2010
Available online 16 October 2010

Keywords:
Titan
Geological processes
Geophysics

ABSTRACT

Cassini RADAR topography data are used to evaluate Titan's hypsometric profile, and to make comparisons with other planetary bodies. Titan's hypsogram is unimodal and strikingly narrow compared with the terrestrial planets. To investigate topographic extremes, a novel variant on the classic hypsogram is introduced, with a logarithmic abscissa to highlight mountainous terrain. In such a plot, the top of the terrestrial hypsogram is quite distinct from those of Mars and Venus due to the 'glacial buzz-saw' that clips terrestrial topography above the snowline. In contrast to the positive skew seen in other hypsograms, with a long tail of positive relief due to mountains, there is an indication (weak, given the limited data for Titan so far) that the Titan hypsogram appears slightly negatively skewed, suggesting a significant population of unfilled depressions. Limited data permit only a simplistic comparison of Titan topography with other icy satellites but we find that the standard deviation of terrain height (albeit at different scales) is similar to those of Ganymede and Europa.

1. Introduction

Although Titan's optical diameter is larger than any other solar system satellite (e.g. Lorenz and Mitton, 2002), the Voyager 1 radio occultation experiment (Lindal et al., 1983) determined Titan's solid-body radius to be 2575 km, relegating Titan to a close second in size behind Ganymede. This zeroth-order metric of topography was key to determining the global density of Titan. Further geophysical studies are enabled by higher-order topographic shape measures – classically a triaxial ellipsoid. Such a shape model for Titan was recently determined (Zebker et al., 2009a).

As more topographic information becomes available, a different way of presenting and considering the information becomes possible, namely hypsometry. A hypsometric profile is essentially[1] the probability distribution of surface height. On the global scale it is influenced by the geological processes at work – notably the Earth's profile is bimodal due to the distinction between oceanic and continental crust. On a local scale the hypsometric profile is used in hydrology (e.g. Strahler, 1962) as a measure of the youth of a surface against erosional processes.

In this paper, we examine the available data to assess Titan's hypsometric profile and its large-scale variations and offer comparisons with other planetary bodies. In addition to its geophysical applications, the hypsogram may also be of use in planning future missions (e.g. balloons) where terrain heights may be a concern. We introduce a variant on the traditional hypsogram, by using a logarithmic abscissa to emphasize the rare extremes of terrain – this highlights some differences in erosion of mountaintops between planets.

2. Hypsometry – a review

The dynamic range of topography is a question that has confronted such historical figures as Plutarch, Laplace and Humboldt, although systematic knowledge of the land and ocean terrain heights was only determined in the late 19th and 20th centuries. The first efforts at quantifying relative areas at different heights was made by Murray (1888) and the first 'modern' hypsogram was constructed by Krummel in 1897. Some notable contributions are discussion of the global hypsogram by Kossinna (1933) and the smaller-scale effect of fluvial erosion on local hysograms by Strahler (1962). Topography data for other worlds were rather sparse in the first decades of the planetary program – one early discussion based on the limited data at the time but showing hypsograms on a comparative basis is that by Head et al. (1977). Orbiting altim-

* Corresponding author.
E-mail address: ralph.lorenz@jhuapl.edu (R.D. Lorenz).

[1] A difference from a simple histogram of heights is that it is conventional to display hypsograms with surface height on the *y*-axis

0019-1035/$ - see front matter © 2010 Elsevier Inc. All rights reserved.
doi:10.1016/j.icarus.2010.10.002

eters (radar or laser) stimulate topographic work, and after the Pioneer Venus mission mapped the topography of much of that planet with a radar altimeter, there was finally a second planetary body with which to compare with the Earth's hypsogram on a near-global basis. One such discussion is that by Head et al. (1982). Magellan data (Ford and Pettengill, 1992) improved the Venus picture a decade and a half later, of course, but the essential features of the hypsogram were indicated by Pioneer Venus.

Somewhat improved terrestrial data, and evolving perspectives on geomorphology, prompted re-examination of the terrestrial hypsogram, e.g. Harrison et al. (1983). Cogley (1985) derives hypsograms for the continental land masses (and the microcontinents Agulhas, Seychelles, Rockall and Jan Mayen) using data at a $1 \times 1^\circ$ resolution, and estimates for the subglacial topography beneath the Antarctic and Greenland ice sheets. That work also notes that the hypsograms are poorly fit by Gaussian curves because they tend to comprise three populations of terrain, a high and a low-altitude 'tail' as well as the main peak. It also notes that Arabia and Africa have hypsogram shapes similar to, but displaced upwards from, other continents, perhaps due to incipient rifting or hotspot epeirogeny.

Much of the interest in hypsography in recent decades, e.g. Wyatt (1984) and Algeo and Seslavsky (1995), has centered on the sensitivity of land area to sea level changes – this has ramifications for such issues as carbon burial. A fundamental property, noted by Cogley and others, is the correlation between the area of continents and their mean height. Numerical models of the balance between tectonism and erosion (e.g. Zhang, 2005) attempt to reproduce this correlation.

The Mars Global Surveyor mission transformed our perspective of that planet by providing, via the Mars Orbiter Laser Altimeter (MOLA) experiment, a global, high-quality topographic dataset that enabled quantitative process-based comparisons with Earth. Smith et al. (1999) note that the apparently bimodal Mars hypsogram may be viewed as an offset between the center-of-mass and center-of-figure of the body. Aharonson et al. (2001) demonstrated this could arise from a discrete topographic step in the presence of noise, and hence cannot alone serve as a test for the long-wavelength nature of the hemispheric dichotomy. Comparison with Earth's ocean-continent bimodality highlights that the test depends on the geographic distribution of the highlands/lowlands. The MOLA dataset also allowed the detection of buried impact structures with surface expressions too subtle to be evident in imagery data, e.g. Buczkowski et al. (2005).

More recently still, topographic data at the Earth has improved. A recent interesting result, facilitated in part by the generation of a near-global uniform, high-resolution and high-quality topographic product from the Shuttle Radar Topography Mission (SRTM) is the latitude-dependent 'cap' on surface height, an effect informally referred to as the 'glacial buzz-saw' (Egholm et al., 2009). Specifically, an upper bound on topographic height appears to be defined by the snowline plus 1500 m, with the snowline at cooler high latitudes occurring at lower elevations.

Recent discoveries at Titan show a world with many physical similarities (geomorphological and meteorological) to the Earth, despite its very different bulk composition and temperature. Titan's elevation statistics merit examination since its terrain presumably represents a balance of mountain-building and erosion analogous to that of Earth, Mars and Venus. Although the topographic data are very incomplete, there is now enough coverage at hand to make a preliminary comparison possible.

3. Titan topographic data

Titan's thick, hazy atmosphere prevents the application of optical limb-profile and stereoscopic methods usually used to generate topographic data on outer solar system satellites. Several types of radar data, however, provide topographic information. On small scales, radarclinometry, i.e. the slope-dependent observed brightness of features with assumed uniform scattering properties can be used to estimate slopes and heights of discrete features (e.g. of mountains, Radebaugh et al., 2007, and of dunes, Lorenz et al., 2006; Neish et al., 2010): in selected areas analogous photoclinometric measurements have been possible in the near-infrared (e.g. Barnes et al., 2008). Additionally, the geometric distortion ('layover') in radar imaging of symmetric structures can be exploited to estimate heights (in effect this is stereo, relying on assumed symmetry for a view of the opposite side) – this was performed e.g. to estimate the depth of the Sinlap crater at 1300 m (Elachi et al., 2006). SAR imaging can also provide topographic information via stereo, where multiple swaths overlap (Kirk et al., submitted for publication). These various topographic measures are rather isolated, having not been systematically obtained over wide areas, and thus are of limited utility for global studies.

On larger scales, radar altimetry along a number of short tracks (~300–700 km long, Zebker et al., 2009b) has been obtained, plus one long one (T 30, 3600 km; a second long altimetry swath was acquired by the spacecraft on T 60 in August 2009 but was lost due to a Deep Space Network (DSN) outage). Slightly longer-than-normal altimetry tracks (800 km and 1200 km) were acquired on T 49, targeted specifically to cover Ontario Lacus (Wye et al., 2009; Wall et al., 2010). The synthetic aperture radar (SAR) imaging swaths are much more extensive, covering approximately 35% of Titan's surface with narrow swaths a few hundred km wide. An along-track topographic estimate profile, referred to as 'SARtopo', can be generated by a monopulse technique exploiting the overlap in the beam footprints that form the swath to estimate the terrain height in several bands along the length of the swath (Stiles et al., 2008). With knowledge of the power distribution within each beam, and knowledge of the spacecraft attitude, the three-dimensional position of the overlap point may be determined.

The topography data is densely sampled along many SAR swaths, but these leave extensive regions of Titan unobserved (see Fig. 1). The coverage of Titan by Cassini RADAR, supplemented perhaps by a few (<10) radio occultation point heights may be expected to improve somewhat beyond the data presently at hand. However, the improvement from measurements in the planned Cassini Solstice Mission will be modest (at best doubling the number of samples) and will not be complete for another 8 years. Thus a preliminary assessment is in order now. A global, high-quality regular gridded topographic dataset for Titan must await a dedi-

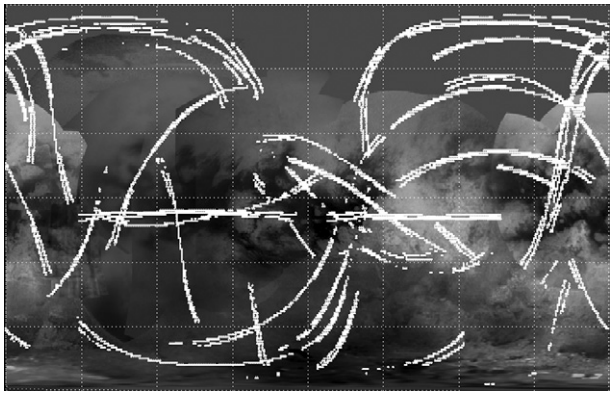

Fig. 1. SARtopo data (where data exist, the $1 \times 1^\circ$ square containing it is plotted in white) overlain on a cylindrical projection basemap of Titan's 940 nm surface reflectivity derived from Cassini ISS images. The leading-face bright region Xanadu is evident at center-right. While far from regularly distributed, the data sample all latitudes and longitudes to at least some degree.

cated Titan orbiter such as those considered in recent NASA studies (e.g. Lorenz, 2009).

4. Data analysis and result

To compute hypsograms, we first populate an array of latitude/longitude/elevation with the data from the SARtopo profiles. The mean value of the elevation data within each latitude/longitude cell is then computed. The present SARtopo dataset already generated (through T 61) comprises well over a million datapoints – the image overlap areas (although reported every ~250 m along-track, the correlation region used by default is ~10 km across, and so the datapoint represents an average elevation of that region) from which the height values are generated (with an estimated precision of ~75 m, Stiles et al., 2008) cover about 1.3% of the area of Titan. When distributed into a $1 \times 1^\circ$ array, about 10% of the 64,800 cells in the global array are populated. (About 34% of the cells of a $5 \times 5^\circ$ array would contain at least some data). All latitudes are sampled to a reasonable degree (Fig. 1) although with a slight emphasis on ~10°S where data from several equatorial flybys (T 8, T 13, T 61) have accumulated. We acknowledge that the computation of a hypsogram from the average heights of $1 \times 1^\circ$ cells entails some loss of information, in that the extremes of topography within each cell are averaged out: however, the comparison datasets we discuss are also $1 \times 1^\circ$ averages, and most of the SARtopo data has in any case an intrinsic resolution not much better than 1° (44 km).

The original surface heights measured by the radar are referenced to Titan's center-of-mass and an assumed radius of 2575 km. We correct the data to the recently published degree-2 geoid of Titan (Iess et al., 2010) using their reference ellipsoid radii a, b, c of 2574.97, 2574.66 and 2574.56 km respectively). It should be noted that the SARtopo technique relies on adequate backscatter strength to make the height correlation: the surfaces of lakes and seas are generally too dark to yield a height. Thus neither the sea surface, nor the sea bed, contributes to the measured hypsogram.

The resultant hypsogram is shown in Fig. 2, with both the raw and geoid-corrected data. It is seen (as noted in Zebker et al. (2009a)) that the data all fall within a range of about 2 km, i.e. 0.1% of Titan's radius. The hypsogram is unimodal. It can also be seen that the hypsogram is slightly narrower with the geoid correction taken into account. The corrected and uncorrected data are also given in Table 1.

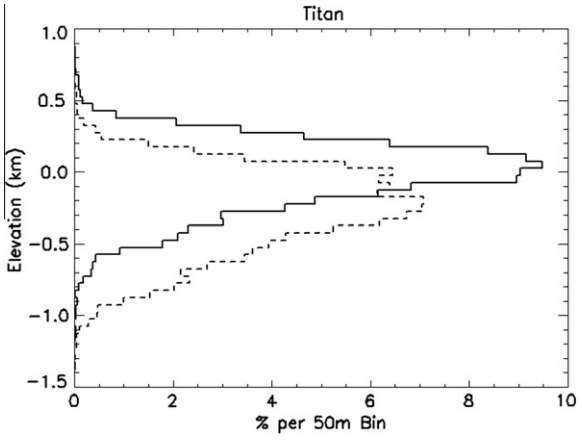

Fig. 2. Titan hypsogram based on all the available SARtopo data. The dashed line represents the raw surface height measurements relative to a 2575 km sphere – it can be seen that the mean value is slightly lower than 0, thus the mean radius in the SARtopo data is about 2574.8 km. The solid line is corrected for the geoid by Iess et al. (2010). The corrected curve is narrower, since the geoid reflects much of the same oblateness seen in the topography data. Note that the hypsogram lacks significant contribution from the liquid surfaces on Titan which are generally too radar-dark to permit a correlation for a SARtopo height estimate.

Conclusions from a hypsogram generated from data covering only 10% of the body must be considered tentative. However, while the map contains some significant gaps, all latitudes and longitudes are sampled to at least some extent (a goal in designing the observations), and both bright and dark terrains are observed, so major sampling biases can be excluded. 1.3% coverage (or, indeed 10%), if widely dispersed as for the RADAR coverage by long, narrow swaths, is adequate to sample global surface properties (e.g. the Titan and Venus global impact crater populations were reasonably well estimated on the basis of 10–15% coverage – Lorenz et al., 2007). However, it is obvious that a terrain that covers only 1% of Titan's surface, has only a small chance of being captured by the present data unless the terrain has a low fractal dimension such that it cannot 'hide' in the gaps between data swaths.

The simple experiment of windowing Earth or Mars topographic datasets with the SARtopo coverage gives an indication of the robustness of the data and conclusions from it. The terrestrial bimodal hypsogram is accurately recovered with only Titan-like coverage (although a minor bump in the curve, due to the unsampled Tibetan plateau, is missed). Similarly, if the Titan coverage were applied to Mars, the Hellas basin and one Tharsis peak would be missed, although Argyre and the two other peaks and Olympus would be seen, and the overall hypsogram would be correctly recovered.

5. Discussion and comparison with other planetary bodies

Useful comparisons with Titan's hypsogram can only be made with bodies for which suitable global topography is available. We further limit ourselves to substantially spherical planetary bodies (i.e. although shape models for a number of small and irregular satellites and asteroids have been made, the comparisons are not likely to be meaningful). This leaves us with Venus, Mars, the Earth and the Moon. The topographic datasets (see Appendix for data

Table 1
Hypsometric data for Titan (data plotted in Fig. 2).

Elevation (m)	Area (corr.) (%)	Area (uncorr.) (%)	Elevation (m)	Area (corr.) (%)	Area (uncorr.) (%)
−1500	0.00	0.00	−250	4.26	7.05
−1450	0.00	0.00	−200	4.87	7.08
−1400	0.00	0.00	−150	6.16	6.13
−1350	0.01	0.01	−100	6.82	6.39
−1300	0.00	0.01	−50	8.97	6.16
−1250	0.00	0.00	0	9.04	6.45
−1200	0.00	0.04	50	9.48	5.48
−1150	0.01	0.05	100	9.15	3.44
−1100	0.02	0.11	150	8.39	2.42
−1050	0.00	0.28	200	6.40	1.51
−1000	0.02	0.46	250	4.65	0.54
−950	0.02	0.47	300	3.38	0.43
−900	0.06	1.00	350	2.07	0.19
−850	0.02	1.53	400	0.84	0.06
−800	0.09	2.01	450	0.37	0.06
−750	0.18	2.32	500	0.16	0.00
−700	0.34	2.15	550	0.12	0.04
−650	0.36	2.69	600	0.08	0.02
−600	0.42	3.45	650	0.08	0.00
−550	0.92	3.62	700	0.03	0.00
−500	1.78	3.94	750	0.01	0.00
−450	2.09	4.28	800	0.02	0.00
−400	2.30	5.24	850	0.02	0.00
−350	3.01	6.18	900	0.00	0.00
−300	2.98	6.73	950	0.00	0.00

sources) have been formatted $1 \times 1^\circ$ to facilitate comparison. There is additionally a hyposgram (Clark et al., 1988) derived from some limited groundbased radar measurements of Mercury (we may expect that knowledge of mercurian topography will improve substantially in coming years with the arrival in orbit of the MESSENGER spacecraft equipped with a laser altimeter and stereo imaging capability – it seems likely that the hypsogram may change appreciably as new data includes coverage of major basins).

These datasets, together with the Titan hyposgram, are plotted in Fig. 3, on the same axes. The narrowness of the Titan hypsogram is striking, as is its unimodality compared with Earth and Mars. Some brief summary statistics of topographic range on the terrestrial planets are given in Table 2. The narrowness deserves some comment. Not only is it narrow in absolute terms, but it is also narrow when normalized to the planetary radius, and even more so when considered in overburden pressure terms (density $\times$ gravity $\times$ height) wherein Titan's gravity and crustal density are both lower than for the terrestrial planets. It is superficially similar in shape and width to the land areas of Earth (perhaps due to the role of fluvial erosion on both bodies) but Titan's hypsogram is noticeably narrower and lacks the long tail due to Earth's (actively-constructed) mountains.

In fact, some consideration of Titan's topography was made prior to Cassini, in order to develop a descent time uncertainty budget for the Huygens probe in order to assure at least 3 min of operation post-impact (one cannot know the time of touchdown if one does not know how high or deep the landing site is). A topographic range of ±2 km was adopted for this purpose, based on analogy with Ganymede, for which some terrain heights had been estimated in Voyager imagery. This estimate seems to have been robustly conservative. Perron and de Pater (2004) discuss the viscous spreading of an ice continent on Titan (stimulated by knowledge of the bright region now known as Xanadu). They find that relief should not exceed 3–7 km. Thus in many respects the Titan hypsogram is narrower than had been expected based on an 'icy satellite geophysics' perspective, again perhaps reflecting the role of fluvial processes.

Table 2
Topographic summary data for $1 \times 1^\circ$ data (all values in km). See text for data sources. Table lists mean radius and ranges that embrace 90%, 80% and 68% of the topographic range, the latter corresponding to the root-mean-squared topographic spread. Titan data are geoid-corrected.

	Radius	90%	80%	RMS
Moon	1738	7.2	5.2	3.9
Earth	6370	6.7	5.8	5.2
Mars	3396	8.2	6.7	5.65
Venus	6051	2.8	1.9	1.35
Titan (corr.)	2575	0.6	0.4	0.25

The asymmetry of the Titan curve is somewhat distinctive in that it is slightly negatively skewed. Whereas the terrestrial body terrains (considering Earth's land area only, and ignoring the more complicated martian situation) have longer tails of positive topography (i.e. the mean is above the mode), this is not the case for the geoid-corrected Titan data. This perhaps indicates the presence of large unfilled depressions on Titan, with comparatively few mountains. It may well be that this negative skew would be yet more prominent if a hypsogram were constructed with estimated surface heights of the liquid-filled basins Ligeia and Kraken Mare, whose sea-beds are not probed by the radar.

Fig. 4 shows the same hypsograms as Fig. 3, but with logarithmic abscissae to emphasize the tails of the distributions. Mars and Venus both have ragged tops, suggesting perhaps construction of mountains that was vigorous compared with the rate of erosion then or since. The top of the terrestrial hypsogram is sharply truncated, evidence of the 'glacial buzz-saw'. A low kurtosis of the Titan

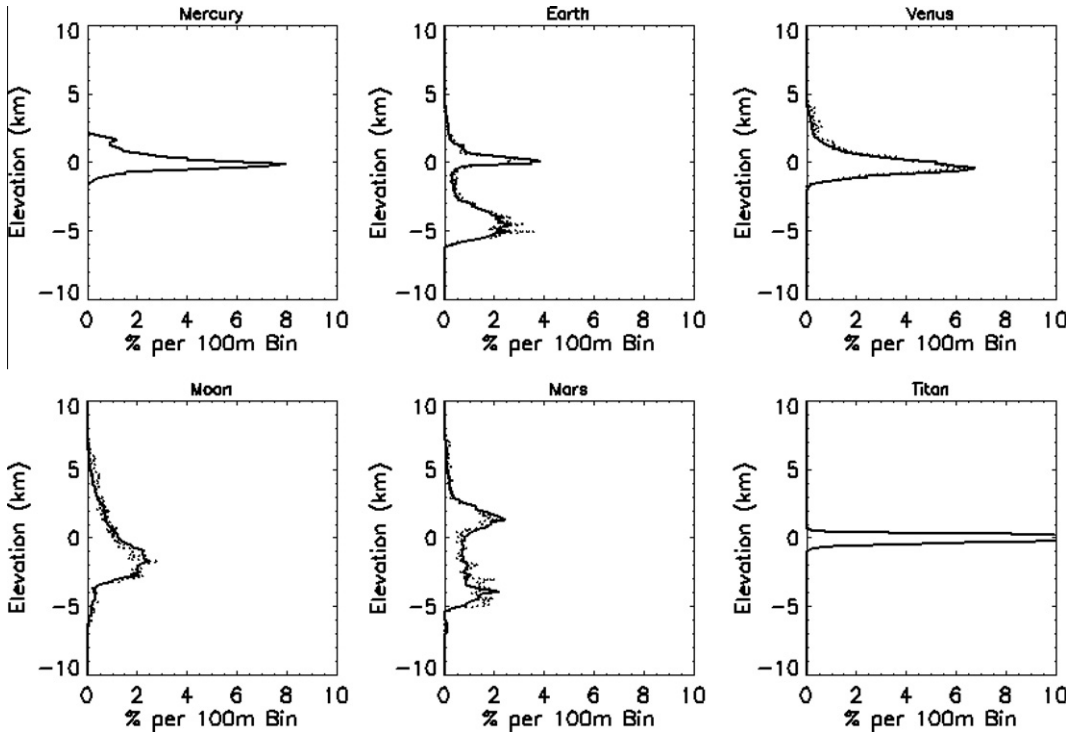

Fig. 3. Planetary hypsograms plotted on the same axes to highlight differences. Notice that most hypsograms are positively-skewed (mountainous terrain leads to a long tail of positive topography, whereas topographic lows tend to be filled in). The dotted curves for Venus, Earth, Moon and Mars show the hypsograms that result if their respective global datasets are sampled with only the coverage that exists for Titan – it is seen that the limited coverage captures the essential differences among these planetary bodies. The extreme narrowness of the Titan hypsogram is evident.

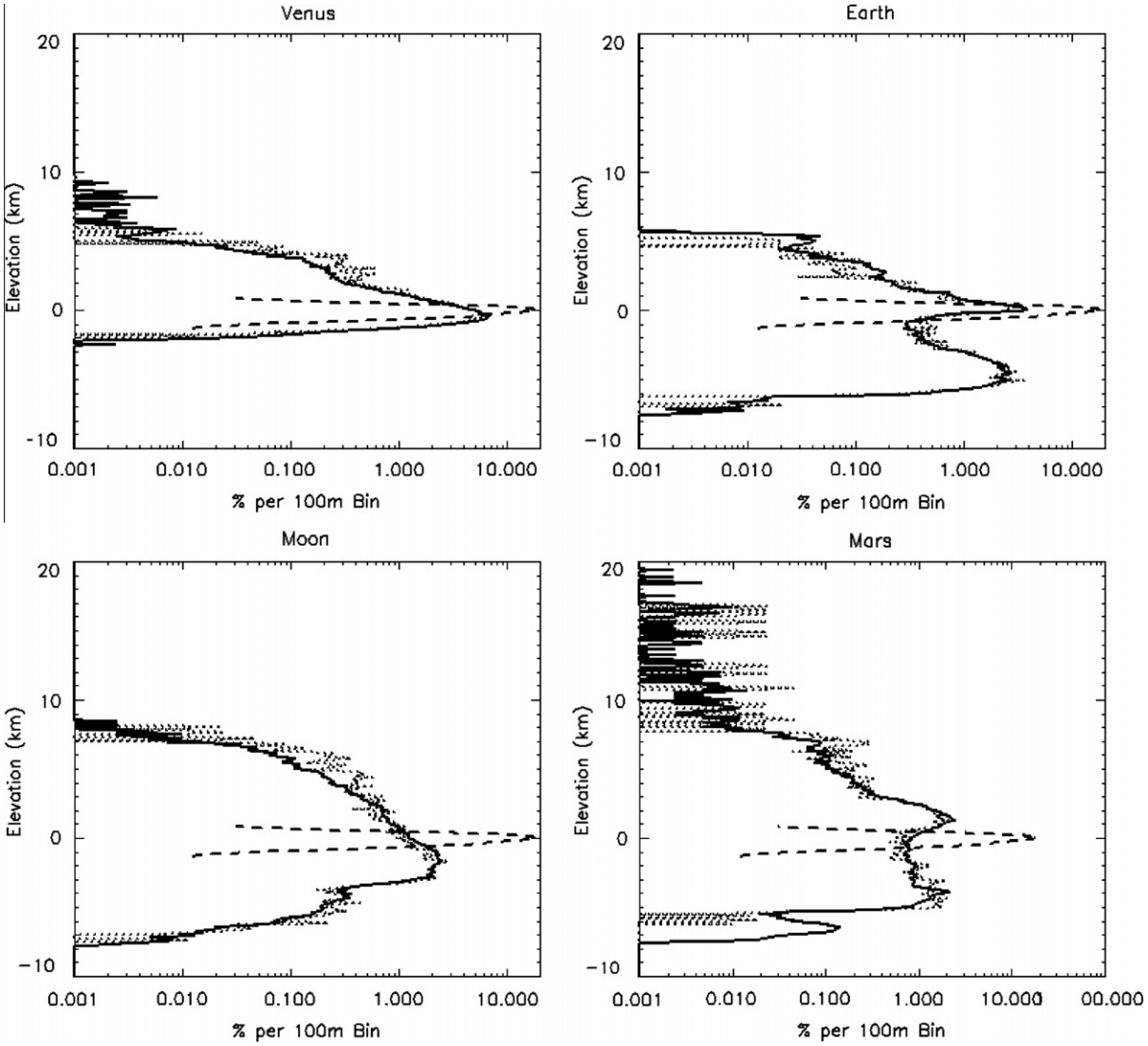

Fig. 4. Hypsograms, this time with logarithmic abscissae and an extended vertical range to emphasize mountains. Titan data are superimposed in dashed line for comparison. Note that the incomplete Titan dataset does not permit accurate assessment of topography covering less than 0.01% of the surface. Mars and Venus both have ragged tops, suggesting perhaps active construction. Although the details are modified slightly for Venus, Earth and Mars by subsampling to the Titan coverage (dotted lines, as for Fig. 3), the existence of the ragged tops overall is not a sampling artifact. The top of the terrestrial hypsogram is sharply cut off, evidence of the 'glacial buzz-saw'. The Mercury data are too sparse to be displayed meaningfully in this representation.

hypsogram (i.e. the sharp top and bottom, with no 'tails') is apparent, indicating a paucity of high peaks and deep depressions, although this is a result that could be modified by future data. It is known that some local topography (e.g. Kirk et al., submitted for publication; Radebaugh et al., 2007) can have ~1–2 km of local relief that is likely averaged out in the $1 \times 1^{\circ}$ array. Although this same averaging applies to the other planetary bodies in Figs. 3 and 4, Titan's mountains do not form large (many square degree) provinces like the Tibetan plateau or the Tharsis volcanos, so the averaging may suppress the tails of Titan's hypsogram more than other bodies. To test this question, we show in Fig. 5 the logarithmic hypsogram constructed from the raw (un-averaged) SARtopo heights. This computation makes no allowance for the overlap between measurements (so areas might formally be in error by a small factor), but does allow some visibility into the extremes of the sampled distribution. The overall shape and narrowness shown in Figs. 2–4 is unchanged, and it is seen that no topography in the SARtopo dataset exceeds 1 km above the geoid. The top of the hypsogram is clipped, somewhat like Earth's. Also notable is that the negative skew is apparent – at the 0.01% level (i.e. of order a

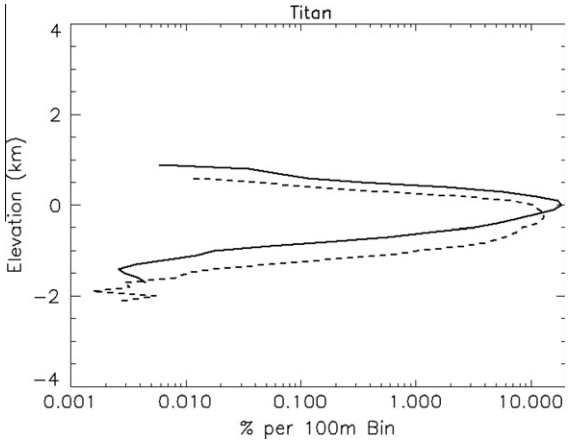

Fig. 5. Titan logarithmic hypsogram constructed from the $\sim 10^6$ raw SARtopo height measurements, uncorrected for overlap. Solid and dashed lines are corrected and uncorrected for the geoid as in Fig. 3. A slight negative tail is evident extending down to −2 km. This tail has no positive counterpart, positive relief not apparently exceeding +1 km.

hundred measurements per bin) there is terrain down to 2 km below the reference surface. We note again that the flooded basin floors of Ligeia and Kraken are not sampled by SARtopo and if they could be seen might stretch the negative tail of the hypsogram even further.

It is seen in these plots that in several places the positive sides of the Earth, Mars and Venus hypsograms are non-monotonic – the decline in area covered by progressively more elevated terrain reverses (at about 5 km on Earth, 6 km on Venus, with weaker inflections at 3 km on Earth and 7 km on Mars). Such inflections in the curve might be considered an indicator of tectonic deformation: a typical shield or cone volcano, or an eroded mountain, will not have such inflections, but rather only a monotonic hypsogram, with progressively more terrain area at progressively lower elevations. Only the generation of a plain at high elevation, by uplift (or perhaps by formation of a flat-topped dome of viscous lava) can produce more fractional area at high elevations than low – the Tibetan plateau is a good example. Notably, the Moon's hypsogram has no such inflections. However, the Titan data are too incomplete to know whether such inflections might be present at the same level as on the terrestrial planets.

Although full topographic datasets for other icy satellites do not presently exist, there are some data on which to base some simple comparisons from stereo and limb measurements. Digital elevation models have been generated over a large part of Iapetus' surface (Giese et al., 2007) and of Uruk Sulcus on Ganymede (Oberst et al., 1999), and limb profiles allow some estimation of the topography of Europa (Nimmo et al., 2007) and the major Saturnian satellites (Thomas et al., 2007). Although hypsograms are not in general available (and the possibility should be borne in mind that limb data may be biased towards positive relief, since depressions may be obscured by adjacent highlands) a root-mean-squared surface height relative to an ellipsoid may be estimated. It should be noted that the icy satellite data are obtained on length scales rather shorter (in general ~1 km) than the somewhat large-scale data for Titan (5–45 km), and this may introduce a bias. For example, Shepard et al., 2001 show that surface height deviations typically vary as the 0.5th power of length scale, at least for 0.01–10 m length scales, although other data e.g. Kirk et al. (2003, 2008) find other variations. Nonetheless, height variance always increases with scale. Broadly speaking, the satellite data are at ~1 km length scales and ~100–1000 km profile lengths, and fall into three main groups. The medium-sized satellites (Rhea, Dione, Tethys) have rms variations of 0.5–1 km, whereas Ganymede and Europa are 0.2–0.5 km (similar to Titan at the 5–45 km scale), and Iapetus is a striking outlier at a Moon-like 4 km. In principle Titan can be considered 'smoother' than Ganymede, but it is difficult to say with the limited data whether the difference between Ganymede and Titan is significant and a fuller exploration of the variation of rms topography with lengthscale is beyond the scope of the present paper.

The relation of geologic history to the hyposgrams of the planets may be summarized in brief as follows. The Moon has substantial topography (principally impact-derived) supported by a strong lithosphere. Large depressions are incompletely filled, leading to a less positively-skewed hypsogram than the other bodies. The generation of the lunar hypsogram by cratering processes was simulated by Sugita and Matsui (1991) – they note that the breadth of the hypsometric curve is strongly influenced by the total number of impact craters, and less so by their size distribution. In this connection it is interesting to note that Titan has relatively few impact craters, as well as a narrow hypsogram.

On Venus, early cratering and possible early plate tectonics might have created more Earth like hypsometry, but lack of ongoing plate tectonics and extensive volcanism has since filled in the lows, giving a positive skew. Erosion is modest, leaving a pronounced high-end tail in the hypsogram. Rosenblatt et al. (1994) suggest that the Venus hypsogram (as indicated by Magellan data) resembles the terrestrial oceanic hypsometric peak and suggest that this is consistent with thermal isostasy on Venus, placing an upper limit of 90 km on the lithospheric thickness if Venus mantle conditions are Earth like.

On Earth, the difference in thickness between continental and oceanic crust presents a bimodality in the hypsogram. Erosion tends to redistribute material to lower elevations, leading to the large peak near sea level, but the bimodality of the hypsogram is maintained in part by the lower density of the continental crust, which allows the crust to buoy upwards isostatically to compensate for erosion. Strong glacial erosion clips the upper end of the hypsogram, and tectonic uplift introduces a couple of inflections. Note that were the oceans not present, unloading of the oceans would cause the ocean basins to rise due to isostasy: thus the oceans have two effects on the hypsogram – creating a near-sea-level peak due to sedimentary deposition and marine erosion, and lowering the elevation of the seabed's hypsometric peak.

On Mars, tectonics and volcanism led to a wide topographic range (retained by a strong crust) with several inflections. Although transport of sediment from the southern highlands into the northern plains may have been significant enough to influence the hypsogram, the presence of many mountain peaks leading to a wide high-end tail in the hypsogram suggests that erosion has been weak since these mountains were constructed.

Thus, in terms of the width of the topographic distribution, in the classic terrestrial sense of a balance between uplift (and/or volcanic construction) and erosion, Titan may reflect a balance wherein erosion wins out more strongly, a balance perhaps also reflected in the rather modest number of impact structures identified on Titan (Lorenz et al., 2007; Wood et al., 2010). Where erosion does not occur, and the crust and lithosphere are stiff enough to retain topography, the hypsogram can be quite wide – as for our Moon and for Iapetus. Titan clearly fails to meet one or both of these conditions.

Lorenz and Lunine (2005) noted the mechanical energy available for erosion and tectonism, exploiting the available geothermal and atmospheric heat flows converted by ideal Carnot engines. For both Earth and Titan, the erosive/atmospheric work exceeded that for tectonism/geothermal work (even allowing for tidal heating of a comparable order to the radiogenic heat flow of ~5 mW/m^2, e.g. Sotin et al., 2009), but a factor of 150 for the Earth but only 15 for Titan, which might naively suggest erosion should be less effective than construction on Titan than on Earth. Thus energetic arguments alone are not obviously able to account for the appearance of Titan. Lack of strength in the lithosphere may be a factor here, constructive processes are somehow weak, or erosion/burial processes may be more effective than energetic would suggest.

6. Conclusions

The first and most important conclusion is that Titan is flat: compared with other planetary bodies for which the relevant data exist, the dynamic range of Titan's topography is very narrow (<2 km) compared with the 10–30 km range seen on Earth, Mars, the Moon and Venus. In the SARtopo dataset, no measured heights exceed the range −2 km to +1 km. We underscore that flat is not the same as smooth – there are nonetheless steep mountains (e.g. Radebaugh et al., 2007) and deep depressions (e.g. Hayes et al., 2008). Slope statistics, and the spatial arrangement of topography and its correlation with other surface properties, will be examined in future work. This narrow hypsogram suggests a number of possible explanations. First, it may be that Titan's lithosphere is too soft or flexible to support large mountain provinces,

and the history of the large rugged, but depressed, Xanadu region is of particular interest in this regard (Radebaugh et al., in press). An alternative possibility is that erosion and sedimentation processes are sufficiently active (relative to impact cratering and mountain-building) to reduce the topographic dynamic range, filling in depressions and eroding down positive relief. The data at hand do not discriminate between these possibilities. Ganymede and Europa do not have atmospheres and thus they lack strong erosive processes, yet at the scale measured apparently have comparable topographic range to Titan: future work will examine the scale-dependence of topographic variation on Titan and elsewhere.

The paucity of impact craters and mountains is consistent with the erosive interpretation. Additionally, many temperate regions of Titan have bland and relatively smooth surfaces, river networks are seen in many parts of Titan, and many craters are degraded, so erosion must occur. It may be that the erosive and/or depositional regimes are latitudinally-dependent.

The Titan hypsogram is slightly negatively skewed, indicating perhaps that depression-forming processes are comparatively strong on Titan relative to the mountain-building processes that give positive skew to the hypsograms of terrestrial bodies. This is, however, a weak result that could be modified by subsequent data.

Acknowledgments

This work was supported by the Cassini–Huygens mission, which is a joint endeavor of NASA, the European Space Agency (ESA), and the Italian Space Agency (ASI) and is managed by JPL/Caltech under a contract with NASA. We are grateful for the cogent criticism of two anonymous referees which improved the paper.

Appendix A. Comparison datasets

In all cases these datasets were averaged to yield a 360×180 array of $1 \times 1^\circ$ heights to permit comparison with Titan on a somewhat equal footing.

The widely-used ETOPO5 dataset was used for the Earth (Data Announcement 88-MGG-02, Digital relief of the Surface of the Earth. NOAA, National Geophysical Data Center, Boulder, Colorado, 1988: downloaded 1/3/2010 from http://www.ngdc.noaa.gov/mgg/global/relief/ETOPO5/) These data are gridded at 5 min (12 pixels per degree) spacing, although in some places the intrinsic resolution is only 1°.

For Venus, a $1 \times 1^\circ$ gridded product (PDS dataset identifier MGN-V-RDRS-5-TOPO-L2-V1.0, downloaded 1/3/2010 from http://pds-geosciences.wustl.edu/missions/magellan/shadr_topo_grav/) was based on Magellan radar altimetry (Ford and Pettengill, 1992). This product contains the measured topography referenced to a sphere of 6051.848 km radius. Since Venus rotates slowly and is not subject to crustally-significant tidal effects, its low-order geoid has a low amplitude and thus does not affect the hypsogram noticeably.

For Mars, a $0.25 \times 0.25^\circ$ gridded product (PDS dataset identifier MGS-M-MOLA-5-MEGDR-L3-V1.0, downloaded 1/3/2010 from http://pds-geosciences.wustl.edu/missions/mgs/megdr.html) based on Mars Global Surveyor (MGS) Mars Orbiter Laser Altimeter (MOLA) data, referenced to an order 60 aroid.

For the Moon, a $1 \times 1^\circ$ gridded product (PDS dataset CLEM1-L-LIDAR-5-TOPO-V1.0, downloaded 1/3/2010 from http://pds-geosciences.wustl.edu/missions/clementine/gravtopo.html). An overall oblateness of 1/3740 is removed from the heights. Terrain poleward of 78° is not covered. Higher quality topographic datasets are now becoming available from the Kaguya and Lunar Reconnaissance Orbiter missions.

References

Aharonson, O., Zuber, M.T., Rothman, D.H., 2001. Statistics of Mars' topography from the Mars Orbiter Laser Altimeter: Slopes, correlations, and physical models. J. Geophys. Res. 106, 23723–23735.

Algeo, T.J., Seslavsky, K.B., 1995. The Paleozoic world: continental flooding, hypsometry and sea level. Am. J. Sci. 295, 787–822.

Barnes, J.W., Brown, R.H., Soderblom, L.A., Sotin, C., Le Mouelic, S., Rodriguez, S., Jaumann, R., Beyer, R.A., Clark, R., Nicholson, P., 2008. Spectroscopy, morphometry, and photoclinometry of Titan's dunefields from Cassini/VIMS. Icarus 195, 400–414.

Buczkowski, D.L., Frey, H.V., Roark, J.H., McGill, G.E., 2005. Buried impact craters: A topographic analysis of quasi-circular depressions, Utopia Basin, Mars. J. Geophys. Res. (Planets) 110 (E03007).

Clark, P.E., Jurgens, R.F., Leake, M.A., 1988. Goldstone radar observations of Mercury. In: Chapman, C.R., Matthews, M.S., Vilas, F. (Eds.), Mercury. University of Arizona Press, Tucson, AZ, pp. 77–100.

Cogley, J.G., 1985. Hypsometry of the continents. Z. Geomorphol., Suppl. 53, 1–46.

Egholm, D.L., Nielsen, S.B., Pedersen, V.K., Lesemann, J.E., 2009. Glacial effects limiting mountain height. Nature 460, 884–888.

Elachi, C. et al., 2006. Titan radar mapper observations from Cassini's TA and T 3 Flybys. Nature 441, 709–713.

Ford, P.J., Pettengill, G.H., 1992. J. Geophys. Res. 97 (E8), 13103–13114.

Giese, B., Denk, T., Neukum, G., Roatsch, T., Helfenstein, P., Thomas, P.C., Turtle, E.P., McEwen, A., Porco, C.C., 2007. The topography of Iapetus' leading side. Icarus 193, 359–371.

Harrison, C.G.A., Miskell, K.J., Brass, G.W., Saltzman, E.S., Sloan, J.L., 1983. Continental hypsography. Tectonics 2, 357–377.

Hayes, A. et al., and the Cassini RADAR Team, 2008. Hydrocarbon lakes on Titan: Distribution and Interaction with a Porous Regolith. Geophys. Res. Lett. 35, L09204.

Head, J.W., Wood, C.A., Mutch, T.A., 1977. Geological evolution of the terrestrial planets. Am. Scientist 65, 21–29.

Head, J.W., Solomon, S.C., Yuter, S.E., 1982. Topography of Venus and Earth: A test for the presence of plate tectonics. Am. Scientist 69, 614–623.

Iess, L., Rappaport, N.J., Jacobson, R.A., Racioppa, P., Stevenson, D.J., Tortora, P., Armstrong, J.W., Asmar, S.W., 2010. Gravity field, shape, and moment of inertia of Titan. Science 327, 1367–1369.

Kirk, R.L., Howington-Kraus, E., Redding, B., Galuszka, D., Hare, T.M., Archinal, B.A., Soderblom, L.A., Barrett, J.M., 2003. High-resolution topomapping of candidate MER landing sites with Mars Orbiter Camera Narrow-Angle images. J. Geophys. Res. 108 (E12), 8088.

Kirk, R.L. et al., and the HiRISE Team, 2008. Ultrahigh resolution topographic mapping of Mars with MRO HiRISE stereo images: Meter-scale slopes of candidate Phoenix landing sites. J. Geophys. Res. 113, E00A2.

Kirk, R.L. et al., submitted for publication. High resolution topographic models of Titan's surface derived by radar stereogrammetry with a rigorous sensor model. Icarus.

Kossinna, E., 1933. Die Erdoberfläche. In: Gutenberg, B. (Ed.), Handbuch der Geophysik, vol. 2. Bornträger, Berlin, Germany, pp. 869–954.

Lindal, G.F., Wood, G.E., Hotz, H.B., Sweenam, D.N., Eshleman, V.R., Tyler, G.L., 1983. The atmosphere of Titan: An analysis of the Voyager 1 radio occultation measurements. Icarus 53, 348–363.

Lorenz, R.D., 2009. A review of Titan mission studies. J. Br. Interplanet. Soc. 62, 162–174.

Lorenz, R.D., Mitton, J., 2002. Lifting Titan's Veil. Cambridge University Press, Cambridge, UK.

Lorenz, R.D., Lunine, J.I., 2005. Titan's surface before Cassini. Planet. Space Sci. 53, 557–576.

Lorenz, R.D. et al., 2006. The sand seas of Titan: Cassini RADAR observations of longitudinal dunes. Science 312, 724–727.

Lorenz, R.D. et al., and the Cassini RADAR Team, 2007. Titan's young surface: Initial impact crater survey by Cassini RADAR and model comparison. Geophys. Res. Lett. 34, L07204.

Murray, J., 1888. On the height of the land and the depth of the ocean. Scott. Geogr. Mag. 4, 1–41.

Neish, C.D., Lorenz, R.D., Kirk, R.L., Wye, L.C., 2010. Radarclinometry of the sand seas of Namibia and Saturn's moon Titan. Icarus 208, 385–394.

Nimmo, F., Thomas, P.C., Pappalardo, R.T., Moore, W.B., 2007. The global shape of Europa: Constraints on lateral shell thickness variations Europa topography. Icarus 191, 183–192.

Oberst, J., Schreiner, B., Giese, B., Neukum, G., Head, J.W., Pappalardo, R.T., Helfenstein, P., 1999. The distribution of bright and dark material on Ganymede and relationship to surface elevation and slopes. Icarus 140, 283–293.

Perron, J.T., de Pater, I., 2004. Dynamics of an ice continent on Titan. Geophys. Res. Lett. 31, L17S04.

Radebaugh, J., Lorenz, R.D., Kirk, R.L., Lunine, J., Stofan, E., Lopes, R., Wall, S., and the Cassini Radar Team, 2007. Mountains on Titan observed by the Cassini RADAR. Icarus 192, 77–91.

Rosenblatt, P., Pinet, P.C., Thouvenot, E., 1994. Comparative hypsometric analysis of Earth and Venus. Geophys. Res. Lett. 21, 465–468.

Shepard, M.K., Campbell, B.A., Bulmer, M.H., Farr, T.G., Gaddis, L.R., Plaut, J.J., 2001. The roughness of natural terrain: A planetary and remote sensing perspective. J. Geophys. Res. 106, 32777–32795.

Smith, D.E. et al., 1999. The global topography of Mars and implications for surface evolution. Science 284, 1495–1503.
Sotin, C., Mitri, G., Rappaport, N., Schubert, G., Stevenson, D., 2009. Titan's interior structure. In: Brown, R.H., Lebreton, J.-P., Waite, J.H. (Eds.), Titan from Cassini–Huygens. Springer, Dordrecht, pp. 61–74. 535pp.
Stiles, B.W. et al., and the Cassini RADAR Team, 2008. Determining Titan surface topography from Cassini SAR data. Icarus 202, 584–598.
Strahler, A.N., 1962. Hypsometric (area-altitude) analysis of erosional topography. Bull. Geol. Soc. Am. 63, 1117–1142.
Sugita, S., Matsui, T., 1991. Evolution of lunar topography by impact processes. Geophys. Res. Lett. 18, 2125–2128.
Thomas, P.C. et al., 2007. Shapes of the saturnian icy satellites and their significance. Icarus 190, 573–584.
Wall, S. et al., 2010. The active shoreline of Ontario Lacus, Titan: a morphological study of the lake and its surroundings. Geophys. Res. Lett. 37, L05202.
Wood, C.A., Lorenz, R., Kirk, R.L., Lopes, R., Mitchell, K., Stofan, E., 2010. Impact craters on Titan. Icarus 206, 334–344.
Wyatt, A.R., 1984. Relationship between continental area and elevation. Nature 311, 370–372.
Wye, L., Zebker, H., Lorenz, R., 2009. Smoothness of Titan's Ontario Lacus: Constraints from Cassini RADAR specular reflection data. Geophys. Res. Lett. 36, L16201.
Zebker, H.A., Stiles, B., Hensley, S., Lorenz, R., Kirk, R.L., Lunine, J., 2009a. Size and shape of Saturn's moon Titan from Cassini Radar altimeter and SAR monopulse observations. Science 324, 921–923.
Zebker, H.A., Gim, Y., Callahan, P., Hensley, S., Lorenz, R., and the Cassini Radar Team, 2009b. Analysis and interpretation of Cassini Titan Radar Altimeter echoes. Icarus 200, 240–255.
Zhang, Y., 2005. Global tectonic and climatic control of mean elevation of continents, and Phanerozoic sea level change. Earth Planet. Sci. Lett. 237, 524–531.